

Mechanistic aspects of the oxidation of phosphines and related substrates by $trans\text{-Ru}^{\text{VI}}(\text{TMP})(\text{O})_2$; TMP = dianion of 5,10,15,20-tetramesitylporphyrin

Stephen Y.S. Cheng, Brian R. James *

Department of Chemistry, University of British Columbia, Vancouver, Canada BC V6T 1Z1

Received 19 April 1996; accepted 15 May 1996

Abstract

The stoichiometric oxidations of some $\text{P}(p\text{-X-C}_6\text{H}_4)_3$ compounds ($\text{X} = \text{OMe, Me, H, F, Cl}$ and CF_3), AsPh_3 and SbPh_3 by $trans\text{-Ru}^{\text{VI}}(\text{TMP})(\text{O})_2$ (**1**) in benzene solution generate the corresponding oxides and $\text{Ru}^{\text{II}}(\text{TMP})(\text{L})$ species ($\text{L} = \text{P}(p\text{-X-C}_6\text{H}_4)_3, \text{AsPh}_3, \text{SbPh}_3$). Stopped-flow kinetic data are consistent with a mechanism involving formation (within a k_1 step) of $\text{Ru}^{\text{IV}}(\text{TMP})(\text{O})(\text{OL})$ which then reversibly dissociates the OL ligand to generate $\text{Ru}^{\text{IV}}(\text{TMP})(\text{O})$; this disproportionates to $\text{Ru}^{\text{VI}}(\text{TMP})(\text{O})_2$ and $\text{Ru}^{\text{II}}(\text{TMP})$, which forms $\text{Ru}^{\text{II}}(\text{TMP})(\text{L})$. ΔH_1^\ddagger values for the phosphine systems vary from 18 to 21 kJ mol^{-1} , increasing with decreasing electron density at the phosphorus, while ΔS_1^\ddagger values become more favorable (-94 to $-78 \text{ J mol}^{-1} \text{ K}^{-1}$) with increasing molecular mass of the substituent. Preliminary kinetic data on the O_2 -oxidations of the substrates catalyzed by (**1**) under 1 atm of air are presented.

Keywords: Mechanism; Phosphine oxidation; Ruthenium

1. Introduction

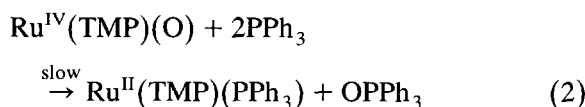
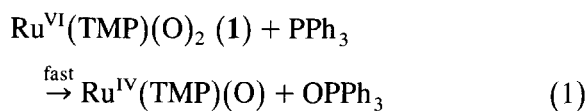
The discovery of $trans\text{-Ru}^{\text{VI}}(\text{TMP})(\text{O})_2$ (**1**) (TMP = dianion of 5,10,15,20-tetramesitylporphyrin), independently by Groves' group [1] and here at UBC [2], has led to some notable catalytic and accompanying coordination and organometallic chemistry [3–5]. Complex (**1**) exhibits a genuine type of dioxygenase activity, where both O-atoms can be transferred to 2 mol equivalents of substrate. O_2 -catalytic systems based on (**1**) include: the oxidation of alkenes to epoxides [3,6], thioethers to sulfoxides [3,7],

and phosphines to phosphine oxides [3,8]. Alcohols can also be catalytically dehydrogenated under air to aldehydes or ketones with generation of H_2O [4], and similarly amines to imines and nitriles [9]. Among the substrates, the phosphine systems are convenient for mechanistic studies of the O-atom transfer reaction from (**1**), and detailed kinetic studies of such systems have not yet been reported. A better understanding of the stoichiometric redox chemistry of (**1**) is crucial for the future development of the catalytic potential of (**1**) and similar dioxygenase-type catalysts.

The oxidation of PPh_3 by (**1**) was initially reported by Groves and Ahn [8]a, the experiments involving $^1\text{H-NMR}$ titrations. Addition of

* Corresponding author.

one equivalent of PPh_3 to (1) gave solely $\text{Ru}^{\text{IV}}(\text{TMP})(\text{O})$ and OPPh_3 , while a further addition of two equivalents of PPh_3 gave $\text{Ru}^{\text{II}}(\text{TMP})(\text{PPh}_3)$ and one more equivalent of OPPh_3 . As no $\text{Ru}(\text{II})$ product was detected during the addition of the first equivalent of PPh_3 , the first 2-electron oxidation by $\text{Ru}(\text{VI})$ was implied to be the faster step, and the second 2-electron oxidation by the $\text{Ru}(\text{IV})$ intermediate to be the slower step



In contrast, kinetic and spectroscopic data on the oxidation of Et_2S to the sulfoxide by (1) were consistent with an initial rate-determining formation of $\text{Ru}^{\text{IV}}(\text{TMP})(\text{O})(\text{OSet}_2)$ followed by a faster step to form $\text{Ru}^{\text{II}}(\text{TMP})(\text{OSet}_2)_2$ [7].

This present paper reports detailed kinetics on the chemistry outlined in Eqs. (1) and (2); the addition of excess OPPh_3 was found to inhibit the rate of reaction (specifically the step shown in Eq. (2)), showing the involvement of coordinated OPPh_3 in the overall process. Mechanisms consistent with the $^1\text{H-NMR}$ and kinetic data, as well as the chemistry of oxoruthenium porphyrin species, are presented.

2. Experimental

The oxidations of $\text{P}(p\text{-X-C}_6\text{H}_4)_3$ ($\text{X} = \text{OMe}, \text{Me}, \text{H}, \text{F}, \text{Cl}$ and CF_3), AsPh_3 and SbPh_3 substrates by (1) were carried out in benzene under 1 atm air. (1) was prepared by aerobically oxidizing the precursor complex $\text{Ru}^{\text{II}}(\text{TMP})(\text{MeCN})_2$ [7,8] in benzene or by adding solid (1) [1,2] directly into benzene. In typical stopped-flow kinetic experiments, $[(1)]$ was $\sim 5 \times 10^{-6}$ M, $[\text{substrate}] \sim 10^{-3}$ M and $[\text{OPPh}_3] \sim 10^{-3}$ M (see Section 3.2 regarding

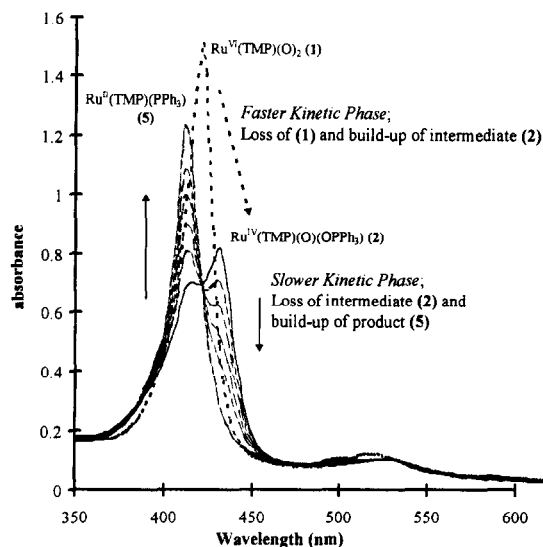


Fig. 1. UV-vis/time traces (HP 8452A) monitoring the conversion from $\text{Ru}^{\text{VI}}(\text{TMP})(\text{O})_2$ (1) (λ_{max} 422 nm) to $\text{Ru}^{\text{II}}(\text{TMP})(\text{PPh}_3)$ (5) (412 nm) at $\sim 20^\circ\text{C}$ in benzene under 1 atm air. In the presence of ~ 0.10 M OPPh_3 , addition of 10 equivalents of PPh_3 forms an intermediate (2) with λ_{max} 430 nm (within seconds), while the product (5) with λ_{max} 412 nm appears over the next 5 min. Isosbestic points are seen at 382, 420, 484 and 538 nm for (2) \rightarrow (5) phase. $[(1)] = 5.4 \times 10^{-6}$ M. λ_{max} nm ($\log \epsilon$ $\text{M}^{-1} \text{cm}^{-1}$) values: (1) 422 (5.45), 516 (4.34); (2) 430 (5.27), 530 (4.28); (5) 412 (5.36) and 504 (4.30) nm.

the general use of OPPh_3 for all the substrates). Purging solutions of (1) and the substrates with Ar gave the same kinetic data as those from the non-deaerated solutions; therefore, anaerobic conditions were unnecessary. Catalytic oxidations of the substrates do occur under air but at much longer time-scales than those of the stopped-flow experiments, where just a net stoichiometric transfer of two O-atoms to two mol equivalents of substrate takes place (see below).

The kinetic data for the phosphine oxidations were collected on a computer coupled to a stopped-flow spectrophotometer (equipment purchased from Applied Photophysics). The overall reaction between (1) and PPh_3 in benzene proceeded via an initial faster kinetic phase ($\sim 10^{-3}$ to 10^{-2} s), followed by a slower one (~ 1 to 10 s). Fig. 1 shows the UV-vis spectral changes for the two-phase reaction. The faster reaction was first-order in (1) and PPh_3 . The slower reaction was first-order in (1), from first-

to zero-order in PPh_3 with increasing $[\text{PPh}_3]$, and the reaction rate was also inhibited by added OPPh_3 . The UV–vis spectra in Fig. 1 were acquired with $[\text{OPPh}_3] = 0.10 \text{ M}$, thus slowing down the loss of the intermediate $\text{Ru}^{\text{IV}}(\text{TMP})(\text{O})(\text{OPPh}_3)$ (**2**), so that it could be observed under non-stopped-flow time-scales (using a Hewlett-Packard HP 8452A Diode-Array Spectrophotometer). Of note, addition of only 1 equivalent of PPh_3 , again under 0.10 M OPPh_3 , rapidly (within seconds) gave (**2**), but no further change was observed in the UV–vis spectrum. The faster reaction was monitored for the loss of (**1**) at its Soret maximum at 422 nm. The slower reaction was monitored at either the 430 or 412 nm Soret maxima, corresponding to the loss of the intermediate (**2**) and build-up of the product $\text{Ru}^{\text{II}}(\text{TMP})(\text{PPh}_3)$ (**5**), respectively.

Preliminary studies on the catalytic O_2 -oxidation of the tertiaryarylphosphines were also carried out. Benzene- d_6 solutions containing $\sim 10^{-4} \text{ M}$ (**1**) were prepared, and their exact concentrations were determined by UV–vis spectroscopy from the known ϵ value of (**1**) [7]. $\text{P}(p\text{-X-C}_6\text{H}_4)_3$ ($\text{X} = \text{Me, H, F, Cl}$) stock solutions ($\sim 0.1 \text{ M}$) were prepared by dissolving appropriate weights of the phosphines (Strem Chemicals) in 1.00 ml benzene- d_6 . The catalysis experiments were carried out in NMR tubes kept at 24°C , and containing initially 0.40 ml of solution containing (**1**), with the tube sealed in air with a rubber septum; the solutions were sometimes purged with 1 atm O_2 for 10 min. Appropriate volumes of the stock phosphine solutions were subsequently injected into the NMR tubes. At the end of $\sim 20 \text{ h}$, the samples were analyzed by $^{31}\text{P}\{^1\text{H}\}$ ($\text{X} = \text{OMe, H, Cl}$ systems) or $^{19}\text{F-NMR}$ ($\text{X} = \text{F}$) spectroscopies (Bruker AC-200E spectrometer), from which the areas of integrations for the resonances of the phosphines and phosphine oxides were used to determine the percentage of the oxide product (pulse delays were varied to ensure reliable integrations). Appropriate blank solutions not containing (**1**) were prepared similarly, and the contributions from the autoxidation ($< 10\%$)

were taken into account in the calculation of the total turnover numbers. Variable temperature ^1H and $^{31}\text{P}\{^1\text{H}\}$ -NMR spectra were acquired on a Varian XL-300 spectrometer; ^1H and $^{31}\text{P}\{^1\text{H}\}$ data are reported relative to TMS and 85% aq. H_3PO_4 , respectively, downfield shifts being positive.

3. Results and discussion

3.1. Faster kinetic phase

Fig. 2 shows some selected absorbance–time traces for the faster kinetic phase of the reaction between (**1**) and excess PPh_3 at 20°C . The inset in Fig. 2 shows the analysis of the first-order absorbance decay due to the loss of (**1**) by the Guggenheim method [10], semilog, and curve-fitting methods, and the results from the three cases are in excellent agreement. Fig. 3 shows the plots of the pseudo-first-order rate constants, k_{obs} , versus $[\text{PPh}_3]$ at various temperatures (10 – 40°C). The rate law for the fast reaction is thus

$$\text{rate} = -\frac{d[(\mathbf{1})]}{dt} = \frac{d[(\mathbf{2})]}{dt} = k_1[(\mathbf{1})][\text{PPh}_3]$$

where k_1 = the 2nd-order rate constant for the first O-atom transfer reaction.

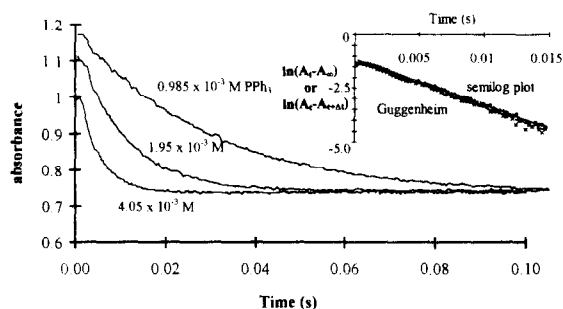


Fig. 2. Absorbance–time traces monitored at 422 nm corresponding to the loss of (**1**) ($4.2 \times 10^{-6} \text{ M}$ in benzene) on reaction with PPh_3 at 20°C , obtained by stopped-flow spectrophotometry. Inset shows the semilog $[\ln(A_t - A_\infty)]$ and Guggenheim $[\ln(A_t - A_{t+\Delta t})]$ plots, where A_t = absorbance at time t , A_∞ = final absorbance, and $\Delta t = 0.0075 \text{ s}$, for the system with $[\text{PPh}_3] = 4.05 \times 10^{-3} \text{ M}$; slope = $-k_{\text{obs}} = -216 \pm 2$, -220 ± 2 and $-227 \pm 2 \text{ s}^{-1}$ by semilog, Guggenheim, and curve-fitting analyses, respectively.

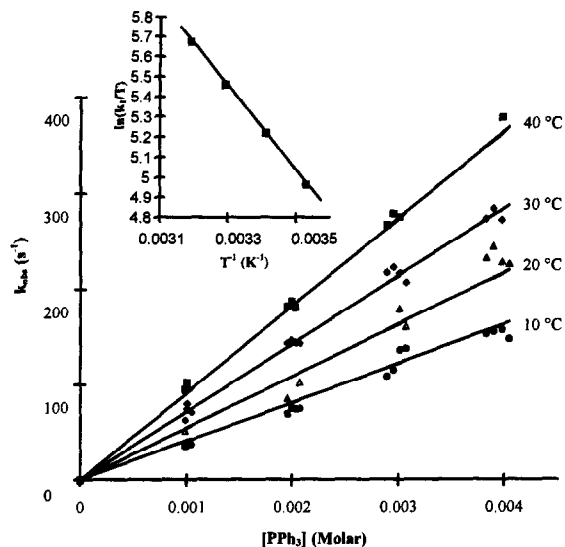
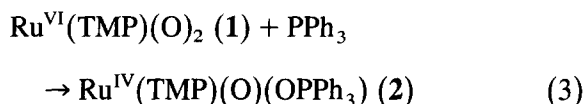


Fig. 3. Plots of k_{obs} versus $[\text{PPh}_3]$. Inset shows the Eyring plot for the k_1 values ($k_{\text{obs}} = k_1[\text{PPh}_3]$).

In this faster kinetic phase, the addition of excess OPPh_3 (up to 10^{-3} M) to the benzene solutions had no effect on the kinetics, showing that OPPh_3 is not involved in the faster reaction. Table 1 lists the k_1 values derived from the slopes of plots such as Fig. 3 for all the substrates, as well as the activation parameters derived from the temperature dependence data (see inset of Fig. 3). As the presence of OPPh_3 slows the reaction rate in the slower kinetic phase (cf. Eq. (2), see Section 3.2), the product

formed in the faster kinetic phase must at least initially be $\text{Ru}^{\text{IV}}(\text{TMP})(\text{O})(\text{OPPh}_3)$ (2), and not $\text{Ru}^{\text{IV}}(\text{TMP})(\text{O})(3)$, although this clearly binds OPPh_3 reversibly, and whether (2) or (3) is detectable depends on $[\text{OPPh}_3]$ (see also Sections 3.2 and 3.3). Hence, the k_1 step refers to Eq. (3)



The ΔH_1^\ddagger and ΔS_1^\ddagger values correspond to the activation parameters for the O-atom transfer reaction from (1) to the substrates studied (cf. Eq. (3)). The ΔH_1^\ddagger values are much lower than for the corresponding, much slower, reactions with some alkyl thioethers ($\Delta H_1^\ddagger \sim 50$ kJ mol $^{-1}$, with k_1 in the range of 0.01–0.10 M $^{-1}$ s $^{-1}$ at 20°C) [7], presumably reflecting the higher nucleophilicity, and ease of oxidation, of phosphines versus thioethers. The ΔS_1^\ddagger values are comparable for the phosphine and thioether systems, showing that the O-atom transfer, coupling, reaction is as expected unfavorable entropically.

In an attempt to understand better the electronic effects of the reaction, the para substituent within the phenyl group of PPh_3 was varied, but it is clear from the data in Table 1 that there is no linear relationship between the

Table 1

Second-order k_1 rate constants and associated activation parameters for the initial O-atom transfer from $\text{Ru}^{\text{VI}}(\text{TMP})(\text{O})_2$ (1), to $\text{P}(p\text{-X-C}_6\text{H}_4)_3$, AsPh_3 and SbPh_3 substrates in benzene

Substrate	σ^a	$k_1 \times 10^{-4}$ (M $^{-1}$ s $^{-1}$)				ΔH_1^\ddagger (kJ mol $^{-1}$)	ΔS_1^\ddagger (J mol $^{-1}$ · K $^{-1}$)
		10°C	20°C	30°C	40°C		
$\text{P}(p\text{-X-C}_6\text{H}_4)_3$							
X = OMe	-0.268	8.14 ± 0.08	10.9 ± 0.02	14.8 ± 0.02	19.2 ± 0.02	18 ± 1	-87 ± 5
X = Me	-0.17	4.29 ± 0.07	5.88 ± 0.07	7.69 ± 0.18	10.0 ± 0.3	18 ± 1	-92 ± 5
X = H	0	3.95 ± 0.14	5.7 ± 0.3	7.18 ± 0.14	9.38 ± 0.15	18 ± 1.4	-94 ± 5
X = F	0.062	7.62 ± 0.13	10.6 ± 0.02	14.2 ± 0.2	18.1 ± 0.4	18.9 ± 1	-84 ± 4
X = Cl	0.227	9.17 ± 0.11	12.8 ± 0.2	16.9 ± 0.2	22.3 ± 0.03	19.4 ± 1.6	-81 ± 5
X = CF $_3$	0.54	6.38 ± 0.17	9.10 ± 0.3	12.7 ± 0.3	16.6 ± 0.4	21 ± 1.4	-78 ± 5
AsPh_3	—	0.0623 ± 0.0007	0.0940 ± 0.0006	0.147 ± 0.001	0.212 ± 0.001	28.7 ± 1	-90 ± 3
SbPh_3^b	—	285 ± 30	—	325 ± 30	—	10.2 ± 2	-85 ± 10

^a σ , the Hammett factor, taken from Ref. [11].

^b k_1 also determined at 15°C (303 ± 35) and 25°C (362 ± 35).

k_1 values for the $P(p\text{-X-C}_6\text{H}_4)_3$ substrates and the Hammett σ factor [11]. Non-linearity observed in the Hammett plot is usually considered to indicate a change in reaction mechanism, but this is unlikely for this series of phosphine substrates. A conventional plot of $\log(k_x/k_H)$ versus σ can be linear only if the change in the para substituent (a purely electronic effect) results in one of the following scenarios [12]: (i) $\Delta H_1^\ddagger = \text{constant}$, implying $\Delta(\Delta S_1^\ddagger) \propto \sigma$; (ii) $\Delta S_1^\ddagger = \text{constant}$, implying $\Delta(\Delta H_1^\ddagger) \propto \sigma$; (iii) $\Delta(\Delta H_1^\ddagger) \propto \sigma$ and $\Delta(\Delta S_1^\ddagger) \propto \sigma$. The data for the phosphine systems fit none of these situations. The ΔH_1^\ddagger values do increase somewhat with increasing electron-withdrawing capacity of the X-groups (Fig. 4) and if one considers an electrophilic attack of a Ru=O moiety of (1) on the lone-pair of electrons on $P(p\text{-X-C}_6\text{H}_4)_3$, then withdrawal of electron density from phosphorus by X should tend to increase ΔH_1^\ddagger .

Of note, no trend is found for ΔH_1^\ddagger on going from PPh_3 to $AsPh_3$ to $SbPh_3$. ΔH_1^\ddagger increases by 50% on going from PPh_3 to $AsPh_3$, while the ΔH_1^\ddagger value for $SbPh_3$ is about half that of the PPh_3 system. ΔH_1^\ddagger is the key factor that primarily governs the k_1 values for the oxidations of EPh_3 ($E = P, As, Sb$), as the ΔS_1^\ddagger

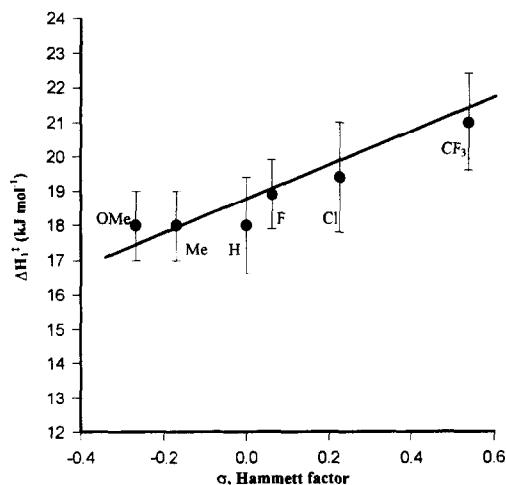


Fig. 4. Modified Hammett plot: ΔH_1^\ddagger versus σ .

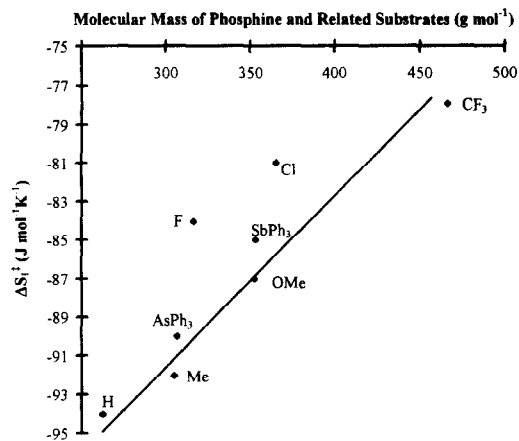


Fig. 5. Plot of ΔS_1^\ddagger versus the molecular mass of phosphine $P(p\text{-X-C}_6\text{H}_4)_3$, $AsPh_3$ and $SbPh_3$.

values are similar in all three cases. Some periodic trends within the series EPh_3 are [13]: the σ donor strength of E decreases in the order $P > As > Sb$; steric effects due to E increase in the order $P < As < Sb$; and steric effects due to Ph decrease in the order $P > As > Sb$. Such effects must govern the ΔH_1^\ddagger values, but no firm conclusions can be drawn based on the current data.

There is no general correlation between ΔS_1^\ddagger and σ , but of interest ΔS_1^\ddagger generally becomes more favorable, i.e. less negative, as the mass of the phosphine, arsine or stibine substrate increases, and an almost linear trend is established (Fig. 5). An earlier suggestion (based on data for the thioether substrates) has been made that if the O-atom transfers are induced via strong Ru=O vibrational coupling [14], the effect is perhaps reflected in a more favorable ΔS_1^\ddagger value with bulkier substrates [7]. Intuitively, one may envision the ΔS_1^\ddagger /mass correlation quantum mechanically in terms of the vibrational energy levels of the transition state, which become closer together (i.e. a larger vibrational partition function, q_{vib} , leads to a more positive $\Delta S_{\text{vib}}^\ddagger$) as the substrate mass becomes larger. Of note, the Tolman cone angles within the series $P(p\text{-X-C}_6\text{H}_4)_3$ are all the same [15], thus ruling out

any possible steric contributions to ΔH_1^\ddagger and ΔS_1^\ddagger ¹.

A nucleophilic attack of the P lone pair on an empty Ru=O π^* -orbital, with the P-atom coordinating to Ru, would be akin to that suggested for O-atom transfer to thioethers within non-porphyrin Ru=O systems [16], but such a mechanism is unlikely here because of the steric demands of the mesityl groups. Also, the 2-electron transfer process accompanying the O-atom transfer is difficult to distinguish from two successive 1-electron transfer steps; however, single-electron transfer processes would not be expected to exhibit such a strong dependence of ΔS_1^\ddagger on substrate mass. The conclusion is that the oxidation occurs as a vibrationally coupled O-atom transfer reaction.

A non-linear Hammett plot has been observed for the stoichiometric oxidation of *p*- and *m*-substituted styrenes by *trans*-Ru^{VI}(porp)(O)₂ (porp = OEP, TPP, the dianions of octaethylporphyrin and *meso*-tetraphenylporphyrin, respectively) [17]. The non-linearity was ascribed to a 'shift' in the electron density on the alkene C=C double bond, as the substituent on the styrene phenyl ring varied from electron-withdrawing (NO₂) to electron-releasing (OMe) groups, and this was thought to change the electronic structure of the transition state. Of note, the Hammett plot was concaving upwards, with the unsubstituted styrene at the minimum of the plot. If there was some change in the electronic structure of the C=C bond, this would not necessarily occur when the substituent was H, although the point was invoked in order to explain the experimental results. A

¹ For a very different substrate, the *non-coordinated* P-atom of the structurally characterize RuCl₂(PPh₃)[*N,N',N''*-P(2-C₅H₄N)₃] of molecular mass 699.48 g mol⁻¹ (R.P. Schutte, Ph. D. Dissertation, University of British Columbia, 1995), $\Delta H_1^\ddagger = 25.7 \pm 1$ kJ mol⁻¹ and $\Delta S_1^\ddagger = -78 \pm 5$ J mol⁻¹·K⁻¹. The ΔH_1^\ddagger value correlates with the presence of an electron-withdrawing substituent (the RuCl₂(PPh₃)-*tris*(pyridyl) moiety), while the ΔS_1^\ddagger value is the same as that for P(*p*-CF₃-C₆H₄)₃, which has the highest molecular mass (466) of the *p*-substituted phosphine substrates.

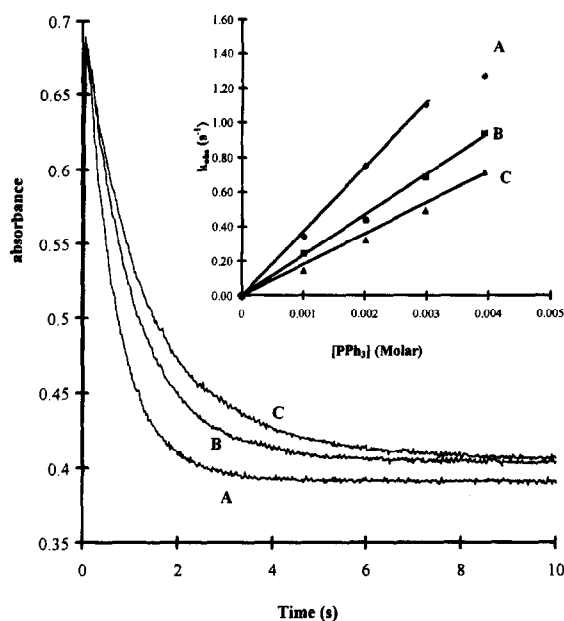


Fig. 6. Absorbance-time traces monitored at 430 nm by stopped-flow spectrophotometry for the slower 2nd step corresponding to the loss of the intermediate Ru^{VI}(TMP)(O)(OPPh₃) (2), via further reaction with PPh₃ (3.9×10^{-3} M, for all three traces) in benzene at 20°C. [(1)]_{initial} = 4.2×10^{-6} M. [OPPh₃] 1.36×10^{-3} M (A), 2.67×10^{-3} M (B) and 3.93×10^{-3} M (C). Inset shows the plots of k_{obs} , derived from these absorbance-time traces, versus [PPh₃] at the different [OPPh₃] values.

look at the activation parameters for the styrene systems might be more insightful.

3.2. Slower kinetic phase

The slower kinetic phase (see Fig. 1), the second part of the overall reaction of (1) with excess PPh₃, is the reduction from Ru(IV) to Ru(II), Eq. (2). That the product is Ru^{II}(TMP)(PPh₃) is discussed in Section 3.3. To obtain kinetic data that analyzed for a pseudo-first-order process, it was necessary to add excess OPPh₃. Fig. 6 shows some absorbance-time traces for the slower second reaction under different concentrations of added OPPh₃ ($\sim 10^{-3}$ M). At the higher [OPPh₃], the pseudo-first-order rate constant k_{obs} shows a first-order dependence on [PPh₃] (Fig. 6, B and C); however, at lower [OPPh₃] there is a hint of a less than 1st-order dependence (Fig. 6A), and

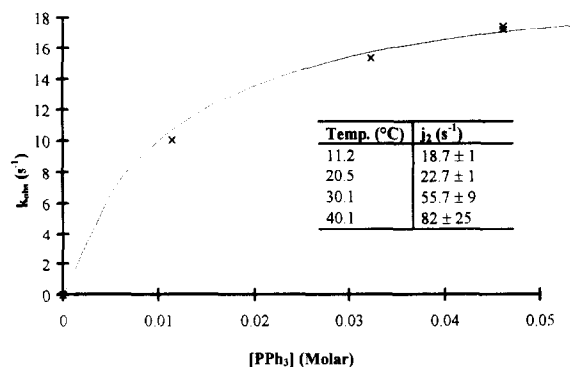


Fig. 7. Plot of k_{obs} versus $[\text{PPh}_3]$ for the kinetics monitored at 430 nm by stopped-flow spectrophotometry for the slower 2nd step corresponding to the loss of the intermediate $\text{Ru}^{\text{IV}}(\text{TMP})(\text{O})(\text{OPPh}_3)$ (2), via further reaction with PPh_3 , in benzene at 20.5°C. $[(1)]_{\text{initial}} = 2 \times 10^{-6}$ M, $[\text{OPPh}_3] = 1.3 \times 10^{-5}$ M. The inset tabulates the values of j_2 at different temperatures.

this was established by studying systems containing much lower added $[\text{OPPh}_3]$ (1.3×10^{-5} M). Fig. 7 shows that the dependence on $[\text{PPh}_3]$ more generally goes from 1st- to zero-order with increasing added PPh_3 , i.e. typical saturation kinetics when $[\text{PPh}_3] \geq 0.05$ M. That OPPh_3 inhibits the reaction (Fig. 6) implies that dissociation of OPPh_3 from $\text{Ru}^{\text{IV}}(\text{TMP})(\text{O})(\text{OPPh}_3)$ (2) is a required step in the process. Two mechanisms (1) and (2) accommodate the observed kinetic dependences.

3.2.1. Mechanism (1)

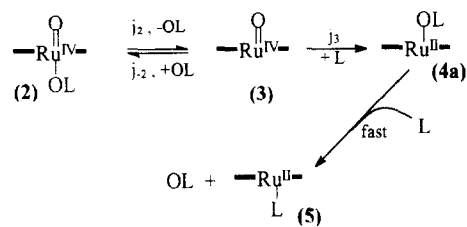
This is similar to that proposed for the thioether oxidations [7]; it involves initial OPPh_3 dissociation from $\text{Ru}^{\text{IV}}(\text{TMP})(\text{O})(\text{OPPh}_3)$ (2), followed by transfer of the O-atom from $\text{Ru}^{\text{IV}}(\text{TMP})(\text{O})$ (3) to PPh_3 to generate $\text{Ru}^{\text{II}}(\text{TMP})(\text{OPPh}_3)$ (4a), and subsequent rapid replacement of the OPPh_3 by PPh_3 to form $\text{Ru}^{\text{II}}(\text{TMP})(\text{PPh}_3)$ (5) (Scheme 1; the rate constants are defined by j_n).

A steady-state treatment applied to species (3) yields the following rate law:

$$\text{rate} = -d[(2)]/dt = d[(5)]/dt = k_{\text{obs}}[(2)],$$

where

$$k_{\text{obs}} = j_2 j_3 [\text{PPh}_3] / (j_{-2} [\text{OPPh}_3] + j_3 [\text{PPh}_3]) \quad (4)$$



Scheme 1. (L = PPh_3)

This rate law is consistent with the described kinetic dependences (Figs. 6 and 7), and the data are readily analyzed using the expression $1/k_{\text{obs}} = 1/j_2 + (j_{-2}[\text{OPPh}_3])/(j_2 j_3 [\text{PPh}_3])$. A plot of $1/k_{\text{obs}}$ versus $[\text{OPPh}_3]/[\text{PPh}_3]$ gives a straight line, with slope $j_{-2}/(j_2 j_3)$ and y-intercept equal to $1/j_2$ (Fig. 8).

The value of j_2 derived from plots such as Fig. 8 is unreliable for these systems because the y-intercept is close to the origin; however, j_2 may be derived from the kinetic data by using the expression $[\text{PPh}_3]/k_{\text{obs}} = [\text{PPh}_3]/j_2 + (j_{-2}[\text{OPPh}_3])/(j_2 j_3)$. A plot of $[\text{PPh}_3]/k_{\text{obs}}$ versus $[\text{PPh}_3]/j_2$ gives a straight line with slope $1/j_2$ (Fig. 9). The temperature dependences of these j_2 values (Fig. 7 inset) do not give a very satisfactory fit to an Eyring plot, which gives $\Delta H_2^\ddagger = 39 \pm 13$ kJ mol⁻¹ and $\Delta S_2^\ddagger = -85 \pm 40$ J mol⁻¹ K⁻¹. The large negative ΔS_2^\ddagger value would thus correspond to the loss of a OPPh_3

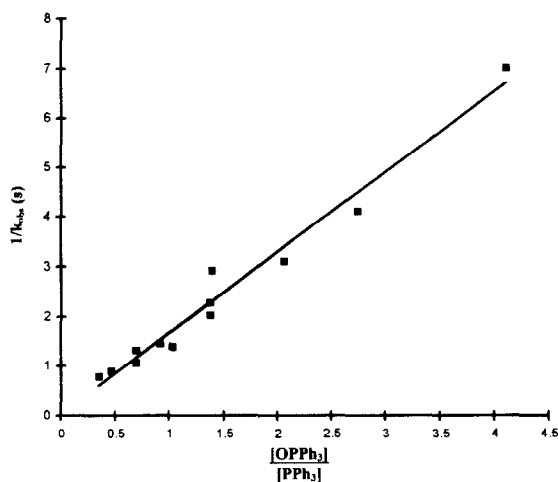


Fig. 8. Plot of $1/k_{\text{obs}}$ versus $[\text{OPPh}_3]/[\text{PPh}_3]$ for data of the type illustrated in Fig. 6. $[(1)]_{\text{initial}} = 4.2 \times 10^{-6}$ M.

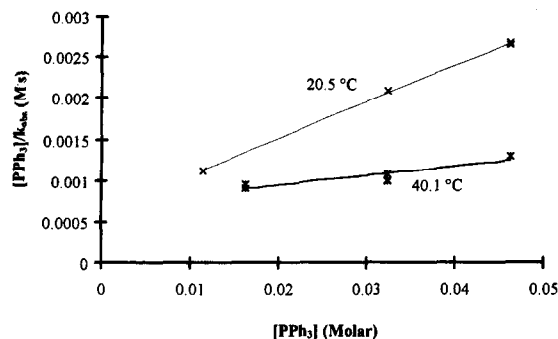
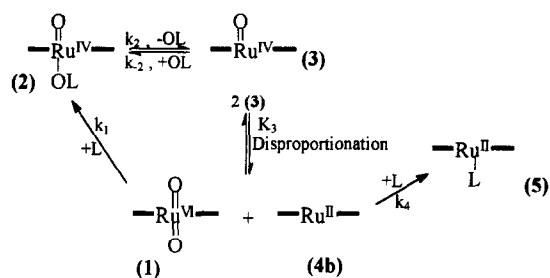


Fig. 9. Plots of $[PPh_3]/k_{obs}$ versus $[PPh_3]$ for data of the type shown in Fig. 7. $[1]_{initial} = 2 \times 10^{-6}$ M, $[OPPh_3] = 1.3 \times 10^{-5}$ M.

from (2), a dissociation reaction; such a finding would require a rationale invoking substantial solvation of the transition state complex which is reasonable if this approximates to the geometry of (3). Mechanism (1) implies that (3) is a more effective O-atom transfer agent than (2).

The data of Figs. 7–9 are readily analyzed to yield j_{-2}/j_3 values, which are summarized in Table 2 for all the $P(p-X-C_6H_4)_3$ systems. The oxidations of all the $P(p-X-C_6H_4)_3$ substrates in the slower kinetic phase were carried out in the presence of added $OPPh_3$; inhibition of the rates with added $OPPh_3$ was always observed implying that once (3) is formed, the j_{-2} step for all the systems involves $OPPh_3$, i.e. this competes successfully (as a ligand for (3)) with the stoichiometric amount of $OP(p-X-C_6H_4)_3$ formed from (2). This is a useful competition kinetic method for it ensures that the varying



Scheme 2. (L = PPh_3)

j_{-2}/j_3 values in Table 2 reflect changes in just j_3 , which defines the rate of addition of the various substrates to the oxo ligand of (3). Unfortunately, the variations in the j_{-2}/j_3 values are small (< a factor of 2 under corresponding conditions), although the data tend to show lower j_{-2}/j_3 values (i.e. higher j_3 values) for the electron-withdrawing X-groups.

3.2.2. Mechanism (2)

An alternative mechanism can be proposed, based on a $Ru^{IV}(TMP)(O)$ disproportionation reaction (Scheme 2). The k_2 and k_{-2} steps are the same as in Scheme 1, but now (3) disproportionates to (1) and $Ru^{II}(TMP)$ (4b), via a rapid K_3 equilibrium. Oxidation of PPh_3 by (1) regenerates (2) (again by the k_1 step discussed in Section 3.1), while ligation of PPh_3 to (4b) gives the product $Ru^{II}(TMP)(PPh_3)$ (5) in a k_4 step. The disproportionation step has been invoked previously for the epoxidation of alkenes [5,6], and dehydrogenation of alcohols [4] and

Table 2

Values for $k_{-2}/(k_2 k_4 K_3^{1/2})$ obtained from the kinetic data for the slower kinetic phase ^a

$P(p-X-C_6H_4)_3$	$k_{-2}/(k_2 k_4 K_3^{1/2})^b$			
	10°C	20°C	30°C	40°C
X = OMe	1.52 ± 0.2	0.92 ± 0.07	0.63 ± 0.08	0.48 ± 0.08
X = Me	2.25 ± 0.17	1.27 ± 0.1	1.05 ± 0.06	0.85 ± 0.07
X = H	2.16 ± 0.2	1.62 ± 0.09	1.26 ± 0.1	1.06 ± 0.1
X = F	1.38 ± 0.06	0.86 ± 0.06	0.63 ± 0.06	0.54 ± 0.05
X = Cl	1.12 ± 0.1	0.69 ± 0.06	0.52 ± 0.054	0.38 ± 0.045
X = CF ₃	1.48 ± 0.3	0.94 ± 0.14	0.44 ± 0.09	0.31 ± 0.07

^a The values correspond to the j_{-2}/j_3 values for analysis of the kinetic data according to mechanism (1) (Scheme 1).

^b k_2 , k_{-2} and $K_3^{1/2}$ are considered to be the same for every reaction (see text). Excess $OPPh_3$ was used in every study to allow for a comparison of k_4 between different phosphine systems.

amines [9] catalyzed by (1), and is almost certainly an essential step in the generation of (1) from the reactions of Ru^{II}(porp) precursors with O₂ [3,7,8]; the 14-electron species Ru^{II}(TMP) has been isolated [2].

The rate law derived from steady-state treatment of (3) is of the same form as that from Scheme 1, but now k_{obs} is given by

$$k_{\text{obs}} = k_2 k_4 K_3^{1/2} [\text{PPh}_3] / \{k_{-2} [\text{OPPh}_3] + (k_1 + k_4) K_3^{1/2} [\text{PPh}_3]\}$$

The analysis of the saturation kinetic behavior (Figs. 7–9) now yields a combination of rate constants $k' = k_2 k_4 / (k_1 + k_4)$, instead of $j_2 (\equiv k_2)$, from the plot of $[\text{PPh}_3] / k_{\text{obs}}$ versus $[\text{PPh}_3]$. If k_4 for the binding of PPh₃ to Ru^{II}(TMP) is $\gg k_1$ (for the nucleophilic attack of PPh₃ on (1)), this k' value would now approximate to k_2 . The Eyring equation applied to k' is not expected to yield a linear plot, and the unsatisfactory Eyring plot obtained for the

j_2 data (see mechanism (1)) provides indirect support for mechanism (2) and the complex k' expression. In mechanism (2), the j_{-2}/j_3 term analyzed within mechanism (1) becomes $k_{-2}/(k_2 k_4 K_3^{1/2})$ (Table 2). The experiments on the various P(*p*-X-C₆H₄)₃ substrates were designed (by exclusive use of OPPh₃ as the inhibiting reagent) so that k_{-2} , k_2 and K_3 are invariable within the different systems, and thus the trends in the $k_{-2}/(k_2 k_4 K_3^{1/2})$ values reflect purely changes in k_4 . As noted earlier the variations are small, but the data are now interpreted to show somewhat higher values of k_4 for the electron-withdrawing X-groups (i.e. for the reaction with the 14-electron species Ru^{II}(TMP)).

The role of an axial ligand *trans* to an oxo ligand in higher valent M=O moieties (M = Fe, Ru) is crucial in dictating oxidation chemistry within biological and/or biomimetic systems [3,7,18,19]. Mechanism (2) (in contrast to mechanism (1)) requires that (3) (containing no ligands *trans* to oxo) preferentially disproportion-

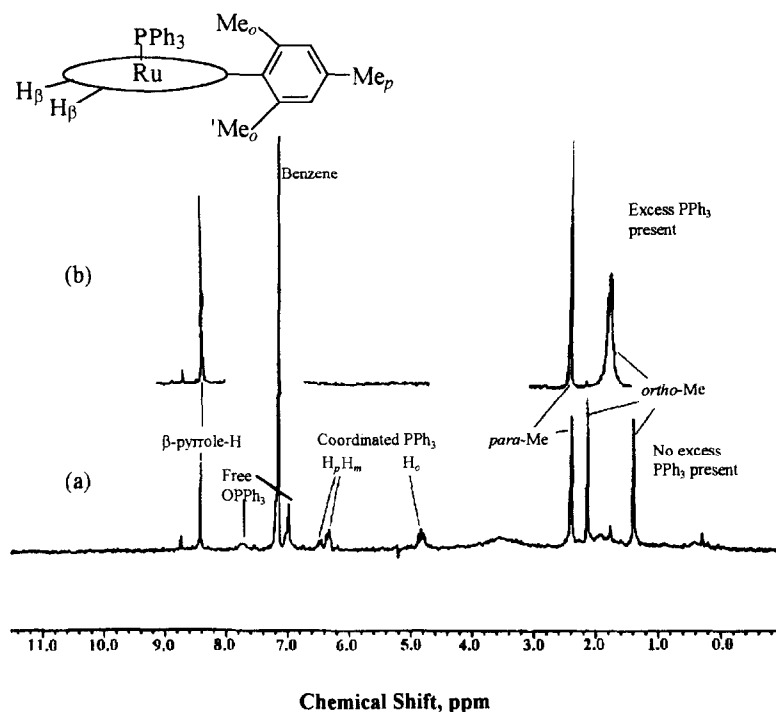


Fig. 10. ¹H-NMR (200 MHz) spectra of Ru^{II}(TMP)(PPh₃) (5) ($\sim 1 \times 10^{-3}$ M) without (a) and with (b) excess PPh₃ in benzene-*d*₆ at 25°C. For (a) (5) was formed from the reaction of (1) and 3 equivalents of PPh₃. For (b) 30 equivalents of PPh₃ were added to (1).

tionates rather than transfers its associated O-atom; the disproportionation step will be favored by the presence of L ligands which ‘siphon off’ the extremely reactive 14-electron species (**4b**) [20] to form (**5**) in the k_4 step. Groves at symposia [21] has reported on exchange data using $^{16}\text{O}_2/\text{H}_2\text{O}^{18}$ systems to show that $\text{Ru}^{\text{IV}}(\text{porp})(\text{O})$ undergoes rapid oxygen exchange with water, while $\text{Ru}^{\text{VI}}(\text{porp})(\text{O})_2$ exchanges slowly, and the findings suggest that the fastest step in catalyzed O_2 -oxidations of, for example, olefins (cf. Scheme 2, where L = an olefin, and (**4b**) reacts with O_2 to form (**3**) [3,5,6]) is the disproportionation reaction. Because of this, and coupled with the reasons noted above, mechanism (2) is strongly favored for the phosphine oxidations. This conclusion perhaps tend to violate the principle of Occam’s razor [22], which liberally interpreted means ‘rationalizing experimental data in terms of the simplest number of steps’. Mechanism (1) with two consecutive O-atom transfer processes is inherently simpler.

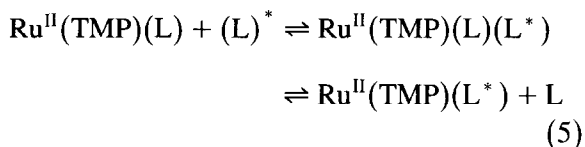
In hindsight, the kinetic data for the thioether oxidations were interpreted in terms of a mechanism akin to that of type (1) (see Introduction) [7]; as in the phosphine system, a disproportionation-type mechanism (cf. Scheme 2) in which L = thioether can also account for the data. The thioether system is currently being re-evaluated.

3.3. The $\text{Ru}^{\text{II}}(\text{TMP})(\text{L})$ product

The stoichiometric ^1H -NMR titrations performed by Groves and Ahn [8]a showed that $\text{Ru}^{\text{II}}(\text{TMP})(\text{PPh}_3)$ (**5**) (along with 2 equivalents of OPPh_3) was the product of the reaction between (**1**) and three equivalents of PPh_3 . We assumed initially that the *bis*(phosphine) complex, $\text{Ru}^{\text{II}}(\text{TMP})(\text{PPh}_3)_2$ would likely form if more than 3 equivalents of PPh_3 were added to (**1**), as $\text{Ru}^{\text{II}}(\text{TMP})(\text{P}^n\text{Bu}_3)_n$ and $\text{Ru}^{\text{II}}(\text{OEP})(\text{PPh}_3)_n$ ($n = 1$ and 2) have been synthesized previously in this laboratory [23]; however, ^1H -NMR and $^{31}\text{P}\{^1\text{H}\}$ -NMR experiments

showed that only (**5**) was formed even when a considerable excess of PPh_3 was used.

Fig. 10 shows the ^1H -NMR spectrum at 25°C of (**5**), the product from the reaction of (**1**) with 3 equivalents of PPh_3 in benzene- d_6 . That two distinct *ortho*-Me ^1H -resonances are observed is indicative of (**5**) possessing C_{4v} symmetry ([7] and [8]a). Of note, the addition of 1 equivalent of PPh_3 to $\text{Ru}^{\text{II}}(\text{TMP})(\text{MeCN})_2$ ([7] and [8]a) yields also (**5**) with the production of free MeCN, and this rules out the possibility of the formation of $\text{Ru}^{\text{II}}(\text{TMP})(\text{PPh}_3)(\text{OPPh}_3)$ (which also possesses C_{4v} symmetry) when (**5**) is produced from (**1**) and PPh_3 . Also shown in Fig. 10 is the ^1H -NMR spectrum of the benzene- d_6 solution of (**5**) formed via the reaction of (**1**) with 30 equivalents of PPh_3 ; the *ortho*-Me protons are now exchange broadened and the signals for the protons of the coordinated PPh_3 have disappeared because of broadening. Rapid PPh_3 exchange at the Ru(II) center causes the broadening (Eq. (5), $\text{L} = \text{L}^* = \text{PPh}_3$), as verified by variable temperature ^1H and $^{31}\text{P}\{^1\text{H}\}$ -NMR studies in toluene- d_8 , on a system containing excess PPh_3 .

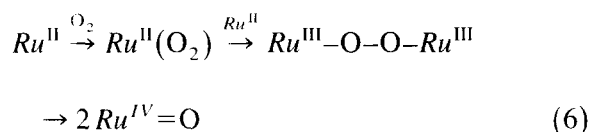


At -78°C , the NMR spectrum resembles that shown in Fig. 10(a); at -40°C , the *ortho*-Me ^1H -resonances appear as a broad, weak, averaged signal, and the PPh_3 resonances are not visible; and at 10°C , the spectrum resembles that shown in Fig. 10(b). At -78°C , the $^{31}\text{P}\{^1\text{H}\}$ -resonance due to the coordinated PPh_3 is observed at δ 35.3; no signal is observed at 10°C . Also, the UV-vis spectrum of (**5**) (Fig. 1) did not change on addition of ~ 0.10 M PPh_3 , further confirming the non-detectability of $\text{Ru}^{\text{II}}(\text{TMP})(\text{PPh}_3)_2$ in solution. Corresponding behavior in the ^1H and $^{31}\text{P}\{^1\text{H}\}$ data are found for the other $\text{P}(p\text{-X-C}_6\text{H}_4)_3$, AsPh_3 and SbPh_3 systems [24].

3.4. Catalyzed O₂-oxidation of P(*p*-X-C₆H₄)₃

Exposure of (5) in benzene-*d*₆ to air, after 2 min, gave Ru^{IV}(TMP)(O) (3) and Ru^{VI}(TMP)(O)₂ (1), with a small amount of (5) remaining, as observed by ¹H-NMR spectroscopy. Free PPh₃ was not observed during the reaction and, within 10 min, OPPh₃ and (1) were the only species in solution. Clearly, this observation accounts, at least qualitatively, for a catalytic air-oxidation of PPh₃ via (1) [3]. For example, with (1) = 2 × 10⁻⁴ M and [PPh₃] = 0.026 M under 1 atm O₂, a total turnover of ~ 30 was obtained after 22 h at room temperature. The turnover frequency ~ 1.4 h⁻¹ corresponds to a much lower rate than for the stoichiometric oxidation of PPh₃ by (1), which is complete within 10 s ([PPh₃] ~ 10⁻³ M). The corresponding catalyzed O₂-oxidations of the X = OMe, Cl and F substrates proceeded similarly with turnover frequencies of up to ~ 3 h⁻¹ over periods of 60 h, but there were no clear trends with substituent effects; indeed, the reaction rates within the NMR tubes are probably governed largely by the diffusion of O₂ from the head-space into the solution.

The catalysis, exemplified by the PPh₃ system, is presumably effected by the observed conversion of Ru^{II}(TMP)(PPh₃) (5) to Ru^{VI}(TMP)(O)₂ (1) under O₂. Considering that the stoichiometric oxidation of PPh₃ by (1) is complete within 1 min and that the exposure of (5) to air, in the absence of excess PPh₃, completely regenerates (1) within minutes, the low catalytic activity must be due to competitive binding of PPh₃ versus O₂ at the vacant site of (5). The latter presumably leads to formation of (1) via the steps outlined in Eq. (6), where Ru = Ru(TMP) or Ru(TMP)(PPh₃) [3,8,25], followed by the disproportionation of the Ru^{IV}=O species.



4. Conclusions

Kinetic data pertaining to the stoichiometric reaction between Ru^{VI}(TMP)(O)₂ (1) and P(*p*-X-C₆H₄)₃, AsPh₃ or SbPh₃ reveal a fast phase involving a single O-atom transfer followed by a slow phase. The O-atom transfer is thought to occur via strong Ru=O vibrational coupling: Δ*H*[‡] is more favorable with increasing electron density at the P-atom, while Δ*S*[‡] is more favorable with increasing molecular mass of the substrate. The kinetic data for the slower reaction can be accommodated within two possible mechanisms: one involves a further, direct O-atom transfer from a Ru^{IV}(O) intermediate, and the other involves disproportionation of the Ru^{IV}(O) intermediate to regenerate (1) and Ru(II). The former mechanism reveals a major role played by the ligand (e.g. OPPh₃) *trans* to the oxo ligand. The disproportionation mechanism is favored because it is more consistent with the general chemistry of other Ru(TMP) systems. The relatively complex behavior within the apparently simple PPh₃/Ru(TMP) system stresses the need for continued research in the area of homogeneous oxidations catalyzed by metalloporphyrins.

Acknowledgements

We thank the Natural Sciences and Engineering Research Council of Canada for financial support, in terms of a Predoctoral Fellowship (SYSC) and research grant (BRJ), and Johnson Matthey Plc and Colonial Metals Inc. for loans of RuCl₃ · 3H₂O.

References

- [1] J.T. Groves and R. Quinn. *Inorg. Chem.* 23 (1984) 3844.
- [2] M.J. Camenzind, B.R. James and D. Dolphin. unpublished work. Oct. 1984; *J. Chem. Soc. Chem. Commun.* (1986) 1137.
- [3] T. Mlodnicka and B.R. James, in: *Metalloporphyrins Catalyzed Oxidations*, F. Montanari and L. Casella (Eds.)

- (Kluwer Academic Publishers, Dordrecht, 1994) p. 121, and references therein.
- [4] S.Y.S. Cheng, N. Rajapakse, S.J. Rettig and B.R. James, *J. Chem. Soc. Chem. Commun.* (1994) 2669; S.Y.S. Cheng and B.R. James, to be published.
- [5] J.T. Groves and J.S. Roman, *J. Am. Chem. Soc.* 117 (1995) 5594.
- [6] J.T. Groves and R. Quinn, *J. Am. Chem. Soc.* 107 (1985) 5790.
- [7] N. Rajapakse, B.R. James and D. Dolphin, *Catal. Lett.* 2 (1989) 219; *Stud. Surf. Sci. Catal.* 55 (1990) 109.
- [8] (a) J.T. Groves and K.-H. Ahn, *Inorg. Chem.* 26 (1987) 3831; (b) P. Le Maux, H. Bahri and G. Simonneaux, *J. Chem. Soc., Chem. Commun.*, (1994) 1287.
- [9] A.J. Bailey and B.R. James, *J. Chem. Soc. Chem. Commun.*, submitted.
- [10] B. Boderie, D. Lavalire, G. Levy and J.C. Micheau, *J. Chem. Ed.* 67 (1990) 459.
- [11] C.D. Johnson, *The Hammett Equation* (Cambridge University Press, Cambridge, 1973) ch. 1.
- [12] P.R. Wells, *Chem. Rev.* 62 (1962) 171.
- [13] F.A. Cotton and G. Wilkinson, *Advanced Inorganic Chemistry*, 5th Ed. (John Wiley and Sons, New York, 1988) p. 432.
- [14] L. Roecker, J.C. Dobson, W.J. Vinning and T.J. Meyer, *Inorg. Chem.* 26 (1987) 779; B.A. Moyer, B.K. Sipe and T.J. Meyer, *Inorg. Chem.* 20 (1981) 1475; A. Dovletoglou and T.J. Meyer, *J. Am. Chem. Soc.* 116 (1994) 215.
- [15] P.B. Dias, M.E. Minas de Piedale and J.A. Martinho Simões, *Coord. Chem. Rev.* 135–136 (1994) 737.
- [16] D.G. Lee and H. Gai, *Can. J. Chem.* 73 (1995) 49.
- [17] C. Ho, W.-H. Leung and C.-M. Che, *J. Chem. Soc. Dalton Trans.* (1991) 2933.
- [18] B.R. James, in: *Fundamental Research in Homogeneous Catalysis*, A.E. Shilov (Ed.), Vol. 1 (Gordon and Breach, New York, 1986) p. 309; J.T. Groves and T.J. McMurry, in: *Cytochrome P-450: Structure, Mechanism and Biochemistry*, O. de Montellano (Ed.) (Plenum Press, New York, 1986) ch. 1; D. Mansuy, *Pure Appl. Chem.* 59 (1987) 759.
- [19] P.E. Ellis, Jr. and J.E. Lyons, *Coord. Chem. Rev.* 105 (1990) 181.
- [20] M.J. Camenzind, B.R. James, D. Dolphin, J.W. Sparapan and J.A. Ibers, *Inorg. Chem.* 27 (1988) 3054.
- [21] J.T. Groves, *Proc. 199th Am. Chem. Soc. Meet., Boston, 1990*, Abstract PETR 60; *Proc. 8th Int. Symp. on Homog. Catal.*, Amsterdam, 1992, Lecture K-6.
- [22] W.M. O’Niel, *Fact and Theory* (Sydney University Press, Sydney, 1969) ch. 4.
- [23] C. Sishta, M.J. Camenzind, B.R. James and D. Dolphin, *Inorg. Chem.* 26 (1987) 1181.
- [24] S.Y.S. Cheng, Ph.D. thesis, University of British Columbia, Vancouver, 1996.
- [25] B.R. James, S.R. Mikkelsen, T.W. Leung, G.H. Williams and R. Wong, *Inorg. Chim. Acta* 85 (1984) 209.